Journal of Medicinal Chemistry

Article

pubs.acs.org/jmc

Acylthiourea, Acylurea, and Acylguanidine Derivatives with Potent Hedgehog Inhibiting Activity

Antonio Solinas,[†] Hélène Faure,[‡] Hermine Roudaut,[‡] Elisabeth Traiffort,[‡] Angèle Schoenfelder,[§] André Mann,[§] Fabrizio Manetti,[†] Maurizio Taddei,*[,†] and Martial Ruat*[,‡]

[†]Dipartimento Farmaco Chimico Tecnologico, Università degli Studi di Siena, Via A. Moro 2, I-53100 Siena, Italy

[‡]CNRS, UPR-3294, Laboratoire de Neurobiologie et Développement, Institut de Neurobiologie Alfred Fessard IFR2118, Signal Transduction and Developmental Neuropharmacology Team, 1 Avenue de la Terrasse, F-91198 Gif-sur-Yvette, France

[§]Laboratoire d'Innovation Thérapeutique, UMR-7200, CNRS—Université de Strasbourg, 74 Route du Rhin, F-67401 Illkirch, France

Supporting Information

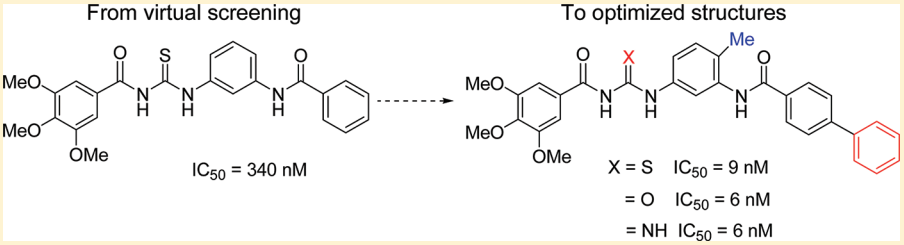

ABSTRACT: The Smoothened (Smo) receptor is the major transducer of the Hedgehog (Hh) signaling pathway. On the basis of the structure of the acylthiourea Smo antagonist (MRT-10), a number of different series of analogous compounds were prepared by ligand-based structural optimization. The acylthioureas, originally identified as actives, were converted into the corresponding acylureas or acylguanidines. In each series, similar structural trends delivered potent compounds with IC_{50} values in the nanomolar range with respect to the inhibition of the Hh signaling pathway in various cell-based assays and of BODIPY-cyclopamine binding to human Smo. The similarity of their biological activities, in spite of discrete structural differences, may reveal the existence of hydrogen-bonding interactions between the ligands and the receptor pocket. Biological potency of compounds **61**, **72**, and **86** (MRT-83) were comparable to those of the clinical candidate GDC-0449. These findings suggest that these original molecules will help delineate Smo and Hh functions and can be developed as potential anticancer agents.

INTRODUCTION

The Hedgehog (Hh) signaling pathway is an essential embryonic signaling cascade that regulates stem and progenitor-cell differentiation in multiple developmental processes. The pathway is also functional in various adult tissues including brain, where its roles are beginning to be explored thanks to the development of genetic and pharmacological tools.[1−3] In mammals, the three Hh homologous proteins Sonic Hh (Shh), Desert Hh, and Indian Hh are present. These homologues differ in their tissue distribution and temporal expression and mediate their activity via a receptor complex composed of two transmembrane proteins, Patched (Ptc), displaying a transporter-like structure, and Smoothened (Smo), presumably belonging to the G protein-coupled receptor family.[4] The repression exerted by Ptc on Smo is relieved when Hh ligands bind Ptc, which leads to a complex signaling cascade involving the transcription factors of the Glioma-associated oncogene (Gli) family and to the activation of target genes including Ptc and Gli themselves.[5,6]

Interruption of Hh signaling during embryogenesis can induce severe developmental defects including holoprosencephaly.[2,7,8] On the other hand, uncontrolled activation of the Hh pathway has been associated with the development of several cancers in both children and adults. Mutation-driven Hh reactivation has been shown to cause basal cell carcinomas and medulloblastomas, whereas alterations in the ligand balance have been associated with onset of pancreatic carcinoma, stomach, esophageal, colorectal, prostate, breast, and liver cancers.[5,6,9] The natural teratogenic compound cyclopamine (Figure 1) blocks Hh signaling by directly binding Smo and slows down the growth of tumors in various animal models,[9,10] thus validating Smo as a therapeutic target in the treatment of Hh-related diseases. Recently, several highly potent Smo antagonists have been described.[11−13] The small-molecule inhibitor GDC-0449 (Figure 1), currently in clinical trials,[14] holds great promise for treating medulloblastomas as well as several Hh-dependent cancers.[6,11−13] However, a Smo mutation arising within the sixth putative transmembrane domain of Smo and disrupting the ability of GDC-0449 to bind Smo, was found in the tumor of a metastatic form of medulloblastoma from a patient who had relapsed after an initial response to the drug.[15,16] A Smo mutation occurring at a homologous position in mouse Smo was also observed in a

Received: October 7, 2011
Published: January 23, 2012

dx.doi.org/10.1021/jm2013369 | J. Med. Chem. 2012, 55, 1559−1571

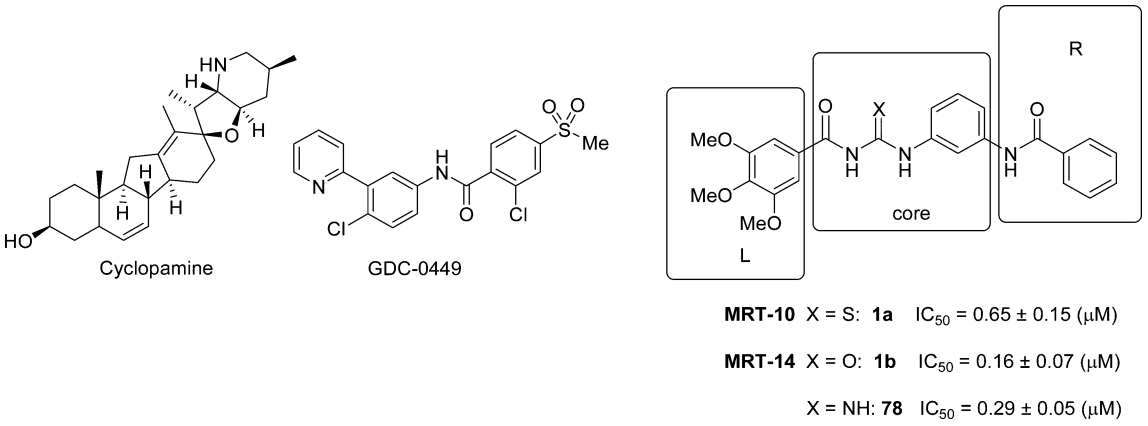

Figure 1. Smoothened antagonists: the scaffolds of AcTU, AcU, and AcG with the three zones (L, core, R) to be explored.

GDC-0449-resistant mouse model of medulloblastoma.[17,18] The development of resistance was also observed in mice exhibiting medulloblastomas treated by the Smo antagonist NVP-LDE225, which has also been progressed into clinical trials.[19] The resistance was associated to either amplification of the transcription factor Gli2, Smo mutations, or up-regulation of the phosphatidylinositol 3-kinase signaling pathway.[19]

Therefore, new ligands are required for characterizing Smo pharmacology in vitro and in vivo and proposing improved drugs for cancer therapy. As a three-dimensional structure of Smo is not yet available, one of the strategies for ligand discovery relies on the screening of large libraries of compounds and subsequent hit optimization. The identification of potent Smo antagonists such as Cur61414 or Z′′′′ was the result of similar efforts.[13,20]

In our ongoing program to identify small molecule inhibitors of the Hh pathway, we developed a ligand-based pharmacophore based on a set of active compounds and carried out a virtual screening of commercial libraries.[20] This approach led us to identify the acylthiourea (AcTU) **1a** (MRT-10 in Figure 1), which displayed an antagonist potency in the micromolar range in various Hh assays (IC_{50} = 0.65 μM on a Gli-luciferase dependent assay, Table 2); the conversion of **1a**, via an oxidative process, into the corresponding acylurea (AcU) produced compound **1b** (MRT-14 in Figure 1), which showed an increased inhibition potency (IC_{50} = 0.16 μM on the same test, Table 4).[20] Furthermore, an additional transformation with HMDS, as nitrogen source, delivered the corresponding acylguanidine (AcG) **78** (Figure 1), which has conserved its ability to inhibit Hh signaling (IC_{50} = 0.29 μM, Table 5).

Whereas AcTU derivatives have shown some benefits for the treatment of solid tumors,[21] AcU compounds, originally developed as insecticides, displayed interesting antitumor activities as shown during random screening.[22] More recently, AcUs have been identified as inhibitors of human liver glycogen phosphorylase[23] and platelet-derived growth factor receptor autophosphorylation,[24] besides as glucokinase activators.[25] AcGs have been recognized as potent ligands for G-protein-coupled receptors. Their improved pharmacokinetic properties over the parent guanidines are attributed to the presence of the acyl residue.[26,27] Therefore, AcTU, AcU, and AcG can be considered as viable scaffolds for medicinal chemistry purposes.

In this paper, we disclose a full account of the chemical post-transformations of the early lead AcTUs compounds into AcUs and AcGs, together with the resulting structure−activity relationships of these new families of Hh antagonists that culminated in the identification of potent Smo antagonists.

RESULTS AND DISCUSSION

From literature indications, it appeared that the acyl-thiourea motif is the ideal substrate for its interconversion into the corresponding ureas or guanidines by simple chemical transformations.[28,29] The structural difference between **1a**, **1b**, and **78** is the nature of their central link, a thiourea, a urea, or a guanidine, respectively. On the basis of the comparable inhibitory potency of the three analogues in two Hh assays, we planned first a structure−activity relationship study on the more easily affordable AcTUs (Figure 1). Then, members of the AcTU series were selected for post-transformations into the desired AcUs and AcGs using standard methods.

Chemistry. The targeted AcTUs were prepared via a classical and convergent sequence. The transient acyl isothiocyanates were obtained by the reaction of selected acylchlorides with ammonium isothiocyanate as partners. Then, the subsequent reactions with different anilines gave the final adducts (Scheme 1 and Supporting Information Scheme 1). The aminoanilides **3a−i**, **5a−l**, **7a−e**, **9a−j**, and **15−19** were obtained from the corresponding 1,3-nitroanilides either prepared following literature reports or purchased directly (Scheme 1). In general, the reduction of the nitro function into amine was performed by transfer hydrogenation with ammonium formate over Pd/C under microwave dielectric heating.[30] This transformation worked efficiently except when a halogen atom was present in any of the two aromatic rings. In these cases, the reduction was performed with $SnCl_2$/HCl/EtOH at 60 °C,[31] leading to the corresponding anilines in good yields (Supporting Information).

Then, acylchlorides A−I (commercially available or prepared from the corresponding acid and oxalyl chloride) were reacted with ammonium isothiocyanate[32] to give the intermediate aroyl isothiocyanates. Finally, they were reacted without purification with the anilines **3a−i**, **5a−l**, **7a−e**, **9a−j**, and **15−19**, followed by 1.5 h of reflux in acetone to give AcTUs **20−67** in acceptable yields from 37% to 77% (Scheme 2). Selected AcTUs **23**, **25**, **30**, **32**, **39**, **41**, **46**, and **60−62** were then transformed into the corresponding AcUs **68−77** by an oxidative process performed with a mixture of CuCl/NaOH under microwave heating, a procedure adapted from reports dealing with oxidation of thioamides and thioureas into the corresponding amides and ureas.[28,33] This method proved to be the most suitable to produce the different AcUs **68−77** (Scheme 2) in variable yields from 32% to 57%. Finally, the

dx.doi.org/10.1021/jm2013369 | J. Med. Chem. 2012, 55, 1559−1571

Scheme 1. The Aminoanilides 3a–i, 5a–l, 7a–e, 9a–j, and 15–19 Obtained from the Corresponding Nitroanilides 2a–i, 4a–l, 6a–e, 8a–j, and 10–14 (For Details Concerning the Preparation of the Nitroanilides 2a–i, 4a–l, 6a–e, 8a–j, and 10–14 Precursors, See Supporting Information Scheme 1)

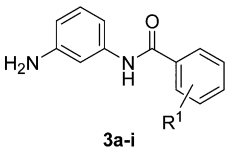

3a-i

a) R^1 = H **b)** R^1 = 2-OMe **c)** R^1 = 3-OMe **d)** R^1 = 4-OMe **e)** R^1 = 2-Cl **f)** R^1 = 4-Cl **g)** R^1 = 4-Ph **h)** R^1 = 3,4,5-OMe **i)** R^1 = 4-F Ph

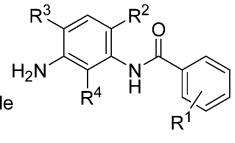

5a-l

a) R^1= R^3 = R^4= H, R^2= Cl **b)** R^1 = R^3 = R^4= H, R^2 = F **c)** R^1= R^3 = R^4= H, R^2 = OMe **d)** R^1= R^2 = R^3 = H, R^4 = Me **e)** R^1= R^2 = R^4 = H, R^3 = F **f)** R^1= 4-F-Ph, R^2= Me, R^3= R^4= H **g)** R^1= R^3 = R^4= H, R^2 = Me **h)** R^3 = R^4= H,R^1= 3-Ph, R^2= Me **i)** R^3 = R^4= H, R^1 = 4-OPh, R^2 = Me **j)** R^1 = 4-Ph, R^2 = Cl, R^3 =R^4 = H **k)** R^1= 4-Ph, R^2 = Me, R^3 = R^4 = H **l)** R^1 = 4-Ph, R^2 = R^3 = H, R^4= Me

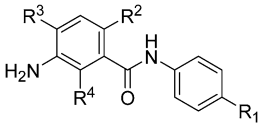

7a-e

a) R^1 = R^3 = R^4 = H, R^2 = Cl **b)** R^1 = R^2 = Cl, R^4 = R^3 = H **c)** R^1 = NMe_2, R^2 = Cl, R^3 = R^4 = H **d)** R^1 = OMe, R^2 = Cl, R^3 = R^4 = H **e)** R^1 = R^3 = R^4 = H, R^2 = Me

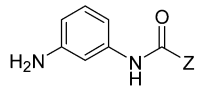

9a-j

a) Z = 4-pyridinyl **b)** = cyclohexyl **c)** = 2-thienyl **d)** = *i*-Pr **e)** = 1-naphtyl **f)** = 2-napthyl **g)** Z = 2-furyl **h)** = 4-morpholino-phenyl **i)** = 4-phenylamino **j)** = 4-Ph-phenylamino

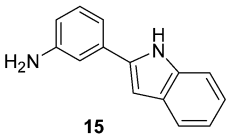

15

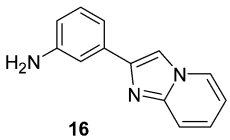

16

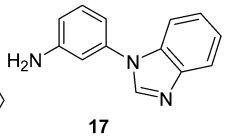

17

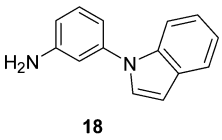

18

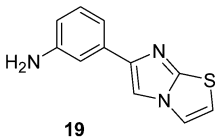

19

Scheme 2. Synthesis of Thioureas, Ureas, and Guanidines[a]

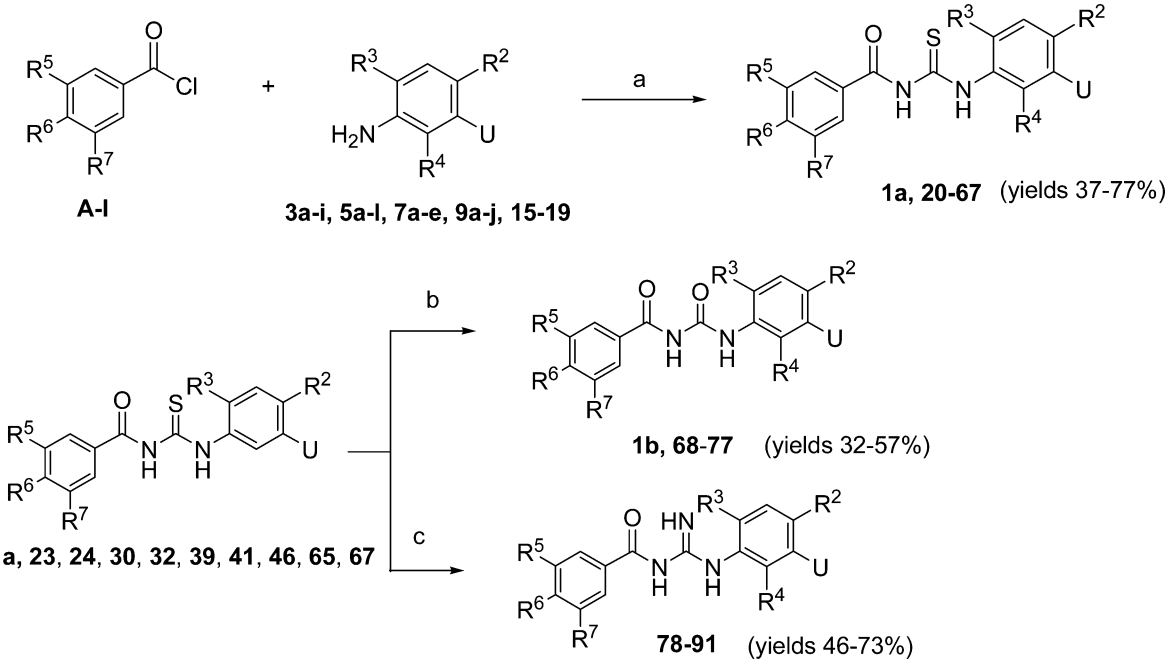

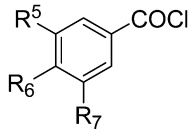

A - I

A): R^5 = R^6 = R^7 = OMe; **B**): R^5 = R^7 = OMe,R^6 = H; **C**): R^5= R^7 = OMe,R^6 = OEt; **D**): R^5 = R^6 = OEt, R^7 = OMe; **E**): R^7 = OMe,R^5, R^6 = -OCH_2O-; **F**): 2-OMe, R^5 = R^6 = H, R^7 = OMe; **G**): R^5= R^6 = R^7 = OEt; **H**): R^5-R^6 = -OCH_2CH_2O-; R^7 = H **I**): R^5 =R^6 = OMe, R^7 = H.

[a]Conditions and reagents: (a) (i) NH_4SCN, acetone, reflux, (ii) addition of anilines **3a–i**, **5a–l**, **7a–e**, **9a–j**, and **15–19**, acetone, reflux; (b) CuCl, NaOH, CH_3CN microwave irradiation; (c) $(Me_3Si)_2NH$, EDCI, CH_3CN, 0°C, 5 h. R^2, R^3, R^4, and U are referring to the appendages explicated in the formulas at the top of the tables.

AcGs **78–91** were obtained from the AcTUs via the corresponding carbodiimides using a mixture of HMDS and EDCI at RT in suitable yields from 46% to 73%.[29] Advantageously, the AcGs can be obtained as hydrochlorides, securing a better solubility. All the final products were produced in acceptable yields, isolated as solids, and could be purified by crystallization in EtOH or *i*-PrOH.

dx.doi.org/10.1021/jm2013369 | *J. Med. Chem.* 2012, 55, 1559–1571

Biological Activity. For structure optimization, the hit molecules were divided in three zones (L, core, and R) as reported in Figure 1. Compounds **20**–**91** were tested for their inhibitory properties in a luciferase reporter assay using Shh as the ligand and Shh-light2 cells, which are NIH3T3 cells stably transfected with a Gli-dependent firefly luciferase reporter widely used for characterizing Hh inhibitors.[34] They were also tested as inhibitors of the differentiation of the mesenchymal pluripotent C3H10T1/2 cells into alkaline phosphatase-positive osteoblasts induced by the Smo agonist SAG.[35,36] In Table 1, the impact on the biological activity of some discrete variations on the L region of the hit molecule is reported.

Table 1. Modifications at the L (Left) Region of the Hit Structure

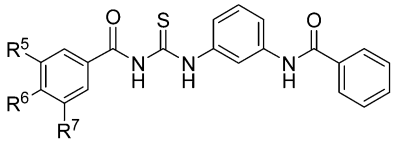

1a: $R^5 = R^7 = R^8$ = OMe; **24**: 2-OMe, $R^5 = R^7$ = H, R^6 = OMe.
20: $R^5 = R^7$ = OMe, R^6 = H; **25**: $R^5 = R^6 = R^7$ = OEt;
21: $R^5 = R^7$ = OMe, R^6 = OEt; **26**: R^5-R^6 = -OCH_2CH_2O-, R^7 = H;
22: $R^5 = R^6$ = OEt, R^7= OMe; **27**: $R^5 = R^6$ = OMe, R^7 = H
23: R^7 = OMe, R^5, R^6 = -OCH_2O-;

	Shh-light2, (Shh 5 nM)	C3H10T1/2, (SAG 0.1 μM)
compound	inhibition, %[a]	IC_{50}, μM
cyclopamine	92 ± 6	0.62 ± 0.03
GDC-0449	100 ± 1	0.011 ± 0.001
1a	96 ± 1	0.9 ± 0.2
20	84 ± 8	1.9 ± 0.2
21	99 ± 2	0.6 ± 0.1
22	100 ± 1	0.8 ± 0.2
23	92 ± 2	1.1 ± 0.6
24	34 ± 4	4.1 ± 0.3
25	100 ± 2	0.8 ± 0.1
26	inactive	nd
27	71 ± 8	nd[b]

[a]At 3 μM; mean ± SEM; $n \geq 3$ for all data; nd: not determined. [b]45% inhibition at 10 μM.

As in further tables, control data relative to cyclopamine, GDC-0449, and **1a** are reported. We decided to maintain an electron-rich aromatic ring with the presence of alkoxy residues. Indeed, variations in the number and the position of the alkoxy substituents on the phenyl ring affected the biological activity. Removal of one methoxyl, independently from the position, resulted in a contrasted impact on the Hh pathway inhibition.

For example, the removal of one methoxy residue in the para position was less detrimental than its removal in the meta position which produced a significant drop in the biological activity (**20** and **27**). If one methoxyl is maintained in para and the second shifted to the ortho position as in AcTU **24**, the activity is also reduced.

The introduction of one, two, or three ethoxy groups in place of the corresponding methoxy resulted in a limited enhancement of the inhibition (see **21**, **22**, and **25**). Interestingly, the triethoxy aroyl group in **25** is also present in SANT-2, a known Hh antagonist.[37] The replacement of the two methoxy groups with a dioxolane ring gave **23** with a decreased activity. Surprisingly, the introduction of a dioxane cycle at the same position produced a completely inactive compound (**26**). From those data, it appears that the presence of the 3,4,5-trimethoxybenzoyl fragment in the L region has a rather beneficial effect on the activity. Therefore, this chemical feature was maintained unchanged in all the following compounds.

The influence of structural modifications at the R region of the hit molecule is reported in Table 2. A phenyl ring in this part of the molecule was required as demonstrated by the low inhibitory properties observed for the cyclohexyl **37** or the isopropyl **39** derivatives or by the presence of thiophene **38** or furan **42** groups (Table 2). Introduction of a methoxy fragment in ortho, meta, or para of the terminal phenyl ring as in **28**–**30** or a chlorine atom in ortho as in **31** has a slightly detrimental effect on the biological activities with respect to the reference compound **1a**, whereas compound **32**, bearing a chlorine atom in the para position, retained the same activity. The presence of a trimethoxy phenyl group in the R zone (as in **34**) was accompanied by a decrease of inhibition in the two assays. Disappointing results were also obtained with the pyridine moiety **36** and with the 1- and 2-naphthalenoyl compounds **40**–**41**, respectively. On the other hand, a major improvement in the inhibition properties was observed with the introduction of a second phenyl ring in para position. Indeed, the biphenyl derivative **33** showed more than 10-fold improvement of the IC_{50} in both assays. The subsequent introduction of a fluorine atom in the para position on the biphenyl ring such as in **35** did not modify the inhibition.

When the second ring was alicyclic (as for **43**), the inhibition dropped. However, if the biphenyl structure is maintained, the replacement of the amide bond with a urea group afforded **45**, which showed a decrease in the inhibition in both assays. A similar manipulation performed on **1a** that provided compound **44** did not greatly modify the inhibition.

Then, the importance of the benzamide group was evaluated by its replacement by iso-electronic or isosteric fragments. For instance, its replacement by an indole fragment led to compound **46**, which displayed a 2–3-fold increased inhibitory activity with respect to **1a**. Other attempts to introduce classical indole isosteres were less productive (see **47**–**50**). The biphenyl derivatives **33** and **35** resulted in the most active compounds in this series. Some conclusions can be drawn from our preliminary investigations: in the L zone, the presence of the electron rich 3,4,5-trimethoxyaryl frame is necessary to maintain the inhibitory potency, whereas in the R region, the introduction of the lipophilic biphenyl fragment has a beneficial impact on the biological activity.

Next, the influence of a central aromatic ring substitution in the core region was explored (Table 3). Modifications on substituents at R^3 and R^2 were first investigated in compounds while maintaining R^1 = H. At R^2, the introduction of a chloro (**51**), fluoro (**52**), or a methyl group (**57**) retained the activity, whereas a methoxyl in the same position (**53**) decreased the inhibition. Compound **51** was the best of this series, with a 3-fold improvement in the inhibitory property with respect to the hit compound in the Shh-light2 assay. At R^3 and R^4, the introduction of substituents did not afford any increment in the activity (**54**–**55**). Then the original amide bond was inverted, leading to compounds **63**–**67**. A significant decrease in the inhibition was observed when comparing compounds **63** and **51**, where the only difference is the reversal of the amide bond. The same observation can also be made for compounds **57** and **67**. However, the introduction of Cl or Me in ortho to the carbamoyl moiety, together with the presence of a biphenyl fragment at R^1, led to **60** and **61**, two compounds with a 3- and 10-fold increase

dx.doi.org/10.1021/jm2013369 | J. Med. Chem. 2012, 55, 1559–1571

Table 2. Modifications at the R (Right) Zone of the Hit Structure

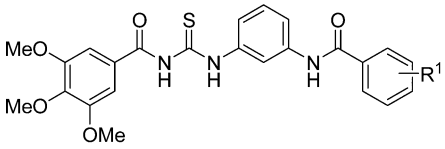

28 R^1= 2-OMe; **32** R^1= 4-Cl;
29 R^1= 3-OMe; **33** R^1= 4-Ph;
30 R^1= 4-OMe; **34** R^1= 3,4,5-OMe;
31 R^1= 2-Cl; **35** R^1= 4-F Ph.

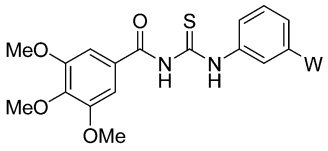

36 W = -NHCO-4-pyridinyl;
37 W = -NHCO-cyclohexyl;
38 W = -NHCO-2-thienyl;
39 W = -NHCO-*i*-Pr;
40 W = -NHCO-1-naphtyl;
41 W = -NHCO-2-napthyl;
42 W = -NHCO-2-furyl;
43 W = -NHCO-4-morpholino-phenyl;
44 W = -NHCONH-phenyl;
45 W = -NHCONH-(4-Ph)-phenyl.

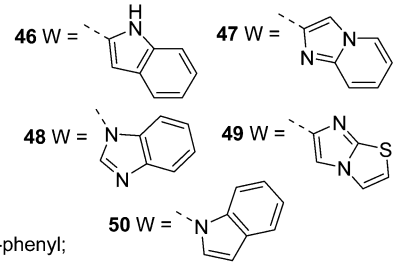

	Shh-light2, (Shh 5 nM)		C3H10T1/2, (SAG 0.1 μM)	
compd	inhibition, %[a]	IC_{50}, μM	inhibition, %[b]	IC_{50}, μM
cyclopamine	92 ± 6	0.3 ± 0.05	98 ± 2	0.62 ± 0.03
GDC-0449	100 ± 1	0.007 ± 0.001	99 ± 1	0.011 ± 0.001
1a	96 ± 1	0.65 ± 0.15	96 ± 4	0.9 ± 0.2
28	49 ± 14	nd	99 ± 6	2.0 ± 0.5
29	99 ± 1	nd	89 ± 3	2.0 ± 1
30	93 ± 3	nd	85 ± 8	1.6 ± 0.3
31	66 ± 11	nd	80 ± 12	2.5 ± 0.6
32	99 ± 1	nd	96 ± 3	0.8 ± 0.4
33	89 ± 1	0.09 ± 0.02	62 ± 3	0.08 ± 0.01
34	37 ± 1	nd	74 ± 7	nd
35	97 ± 1	0.10 ± 0.02	95 ± 3	0.14 ± 0.06
36	67 ± 4	nd	82 ± 8	nd
37	14 ± 13	nd	26 ± 7	nd
38	13 ± 3	nd	60 ± 5	nd
39	6 ± 16	nd	6 ± 4	nd
40	64 ± 10	nd	63 ± 9	nd
41	24 ± 8	nd	59 ± 11	nd
42	53 ± 1	nd	67 ± 12	nd
43	90 ± 5	nd	55 ± 2	nd
44	78 ± 10	nd	104 ± 3	nd
45	71 ± 10	nd	91 ± 1	nd
46	90 ± 4	0.18 ± 0.06	102 ± 1	0.28 ± 0.05
47	93 ± 1	0.82 ± 0.06	94 ± 1	0.55 ± 0.15
48	84 ± 8	nd	60 ± 17	nd
49	92 ± 3	1.1 ± 0.1	98 ± 1	nd
50	69 ± 1	nd	92 ± 7	nd

[a]At 3 μM. [b]At 10 μM; mean ± SEM; $n \geq 3$ for all data; nd, not determined.

in their inhibitory potency compared to **1a**. Maintaining a methyl in the R^2 position and changing the 4-Phe to a 3-Phe or 4-O-Phe in R^1 led to the less potent **58** and **59**. Finally, compound **56**, formally derived from **35** (Table 2) with a Me group incorporated at the R^2 position in the core region, exhibited a 3- to 4-fold further increase in potency in the two assays, confirming the beneficial impact of the methyl in this position. Interestingly, compounds **56** and **61** that differ only by the presence of a fluorine atom on the R^1 phenyl ring display similar activities.

Therefore, the gain in the inhibitory potency with respect to the reference compound may be attributed to the presence of a Cl or a Me substituent at R^2, which partially disrupts the conjugation of the central phenyl and the amide bond. In conclusion, compound **61** was among the most active, showing an IC_{50} = 41 nM in the Shh-light2 assay.

Finally we prepared a set of isosteric ureas to test the influence of this fragment on the biological activity. Some representative AcTUs were transformed into the corresponding AcUs as described in Scheme 2. Interestingly, an increase of the inhibitory properties was observed with most of the AcU structures (Table 4 and Supporting Information Table 2 for correspondence with the AcTU).

Especially for one of the most active compound of our series, the conversion from thiourea (**61**) to urea (**72**) resulted in a substantial gain of potency in the Shh-light2 cells assay (IC_{50} of 41 or 13 nM for **61** and **72**, respectively, in Tables 3 and 4). This effect was more modest when the AcTU **60** was converted

dx.doi.org/10.1021/jm2013369 | J. Med. Chem. 2012, 55, 1559−1571

Table 3. Modifications at the "Core" Region of the Hit Structure

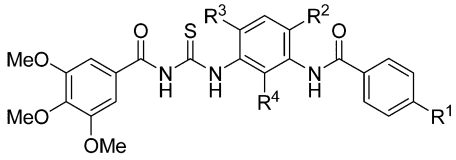

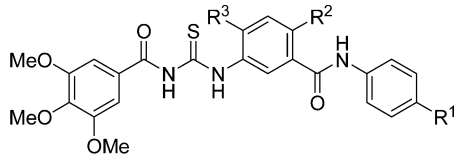

51: $R^1 = R^3 = R^4 = H$, $R^2 = Cl$;
52: $R^1 = R^3 = R^4 = H$, $R^2 = F$;
53: $R^1 = R^3 = R^4 = H$, $R^2 = OMe$;
54: $R^1 = R^2 = R^3 = H$, $R^4 = Me$;
55: $R^1 = R^2 = R^4 = H$, $R^3 = F$;
56: R^1 = 4-F-Ph, $R^2 = Me$, $R^3 = R^4 = H$;
57: $R^1 = R^3$, $R^4 = H$, $R^2 = Me$;
58: $R^3 = R^4 = H$, R^1 = 3-Ph, $R^2 = Me$;
59: $R^3 = R^4 = H$, R^1 = 4-OPh, $R^2 = Me$;
60: R^1 = 4-Ph, $R^2 = Cl$, $R^3 = R^4 = H$;
61: R^1 = 4-Ph, $R^2 = Me$, $R^3 = R^4 = H$.
62: R^1 = 4-Ph, $R^2 = H$, $R^3 = H$, $R^4 = Me$.
63: $R^1 = R^3 = H$, $R^2 = Cl$;
64: $R^1 = R^2 = Cl$, $R^3 = H$;
65: $R^1 = NMe_2$, $R^2 = Cl$; $R^3 = H$;
66: $R^1 = OMe$, $R^2 = Cl$, $R^3 = H$;
67: $R^1 = R^3 = H$, $R^2 = Me$.

	Shh-light2, (Shh 5 nM)			C3H10T1/2, (SAG 0.1 μM)	
compd	inhibition, %[a]	inhibition, %[b]	IC_{50}, μM	inhibition, %[c]	IC_{50}, μM
cyclopamine	57 ± 8	92 ± 6	0.3 ± 0.05	98 ± 2	0.62 ± 0.03
GDC-0449	97 ± 1	100 ± 1	0.007 ± 0.001	99 ± 1	0.011 ± 0.001
1a	15 ± 4	96 ± 1	0.65 ± 0.15	96 ± 4	0.9 ± 0.2
51	69 ± 7	89 ± 4	0.19 ± 0.03	96 ± 3	0.99 ± 0.03
52	21 ± 9	98 ± 1	nd	96 ± 1	nd
53	1 ± 2	33 ± 6	nd	8 ± 1	nd
54	2 ± 2	54 ± 7	nd	44 ± 13	nd
55	4 ± 5	92 ± 8	nd	97 ± 2	nd
56	96 ± 3	97 ± 6	0.029 ± 0.001	86 ± 4	0.03 ± 0.01
57	60 ± 6	100 ± 2	nd	99 ± 1	0.9 ± 0.3
58	72 ± 5	100 ± 1	nd	97 ± 4	0.6 ± 0.6
59	59 ± 1	97 ± 2	nd	99 ± 2	0.5 ± 0.1
60	85 ± 2	99 ± 3	0.13 ± 0.04	101 ± 5	0.38 ± 0.10
61	98 ± 1	98 ± 1	0.041 ± 0.002	100 ± 1	0.06 ± 0.02
62	9 ± 7	48 ± 8	nd	7 ± 13	nd
63	11 ± 5	95 ± 3	0.52 ± 0.09	96 ± 5	1.5 ± 0.1
64	7 ± 7	98 ± 1	nd	96 ± 3	nd
65	4 ± 1	99 ± 1	nd	98 ± 2	nd
66	10 ± 8	100 ± 1	nd	88 ± 1	nd
67	13 ± 5	89 ± 5	1.8 ± 0.6	99 ± 1	2.5 ± 0.5

[a]At 0.3 μM. [b]At 3 μM. [c]At 10 μM; mean ± SEM; $n \geq 3$ for all data; nd, not determined.

to its corresponding AcU **77** (IC_{50} of 130 or 80 nM for **60** and **77**, respectively). More contrasted are the results with the AcTU/AcU pairs **23**/**68** and **25**/**69**: the replacement of the methoxyl-triade (present in **1a**) with other alkoxyl surrogates is detrimental for the corresponding urea. The data showed again that the location of the Me in the central core region was important for inhibition of Hh signaling (compare **72** and **74**). Finally, urea **72** was the most potent compound, confirming the preference for the methyl group over the chlorine atom next to the amide appendage.

As highlighted in the chemical section, the interconversion of an AcTU to an AcG can be obtained in one step via a carbodiimide. Because AcGs could be converted to hydrochlorides, this transformation constituted a convenient way to increase their water solubility. Therefore, the most active AcTUs were transformed into the corresponding AcGs **78**−**91** (see Table 5). As a general trend, AcGs were more potent inhibitors than the AcTUs (compare **78** to **1a** and **86** to **61** and see Supporting Information Table 3) and equipotent to AcUs (compare **78** to **1b** and **86** to **72**, Table 6). Most of the synthesized AcGs displayed inhibitory potency in the nanomolar range (Table 5).

Interestingly, the Smo receptor seemed to accommodate equally the (thio)urea and the guanidine moieties. Albeit the electronic properties at the molecular level are slightly different, the same structural features should equally operate in all series. Furthermore, the presence of a methyl or a chlorine substituent on the central ring (compare **78** to **88** and **89**) and the biphenyl appendage (compare **88** to **85** and **89** to **86**) had a decisive contribution to the biological activity. The addition of a fluorine atom on the biphenyl group as in **84** did not modify the inhibitory properties compared to **86**. The potency of **79** revealed that the contribution of the 2-indolyl over the 1-indolyl nucleus is rather beneficial in this series (compare **79** and **82**). The inversion of the amide bond in **90** and **91** in respect to **89** and **88**, respectively, did not affect the potency. The best compounds were **84** and **86**, with similar potency as the reference compound GDC-0449 and surpassing by far cyclopamine.

Thus from this lead optimization study, decisive structural features can be identified for the AcTU, AcU, and AcG ligands, considered as bioisosteres: (i) the 3,4,5-trimethoxybenzoyl (or triethoxybenzoyl) fragment at the L region, (ii) a 4-Me or 4-Cl on the 1,3-diamino aryl fragment at the central aromatic core, and (iii) a biphenyl appendage at the R region (Scheme 3). The following structural consequences can be drawn: (i) the methyl substituent or the chlorine atom are inducing a torsion of the central phenyl ring with respect to the related amide bond, and

dx.doi.org/10.1021/jm2013369 | J. Med. Chem. 2012, 55, 1559−1571

Table 4. Biological Activities of Acylureas

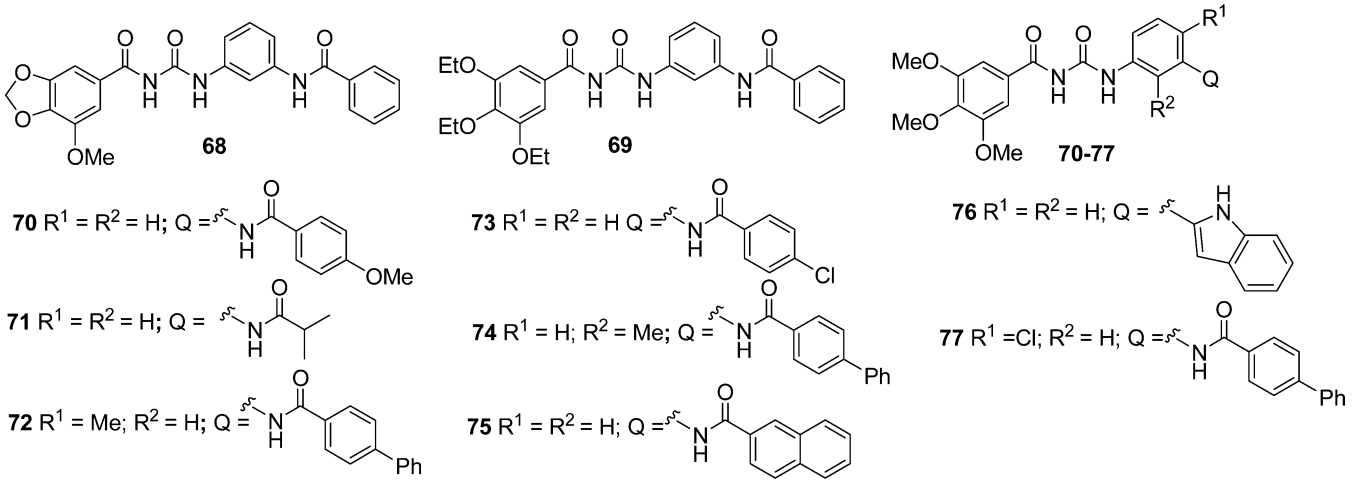

	Shh-light2, (Shh 5 nM)			C3H10T1/2, (SAG 0.1 μM)	
compd	inhibition, %[a]	inhibition, %[b]	IC_{50}, μM	inhibition, %[c]	IC_{50}, μM
cyclopamine	57 ± 8	92 ± 6	0.3 ± 0.05	98 ± 2	0.62 ± 0.03
GDC-0449	97 ± 2	100 ± 1	0.007 ± 0.001	99 ± 1	0.011 ± 0.001
1b	76 ± 5	96 ± 1	0.16 ± 0.07	101 ± 5	0.13 ± 0.05
68	1 ± 4	2 ± 2	nd	32 ± 11	nd
69	13 ± 5	24 ± 11	nd	45 ± 14	nd
70	40 ± 4	103 ± 1	nd	99 ± 1	nd
71	4 ± 4	62 ± 8	nd	99 ± 3	nd
72	96 ± 2	99 ± 1	0.013 ± 0.002	101 ± 3	0.025 ± 0.003
73	6 ± 6	96 ± 1	nd	95 ± 3	nd
74	26 ± 10	99 ± 1	nd	104 ± 1	nd
75	1 ± 7	3 ± 4	nd	4 ± 3	nd
76	85 ± 6	90 ± 5	0.11 ± 0.03	97 ± 1	0.22 ± 0.04
77	95 ± 2	98 ± 1	0.08 ± 0.01	72 ± 4	0.10 ± 0.03

[a]At 0.3 μM. [b]At 3 μM. [c]At 10 μM; mean ± SEM; $n \geq 3$ for all data; nd, not determined.

(ii) the biphenyl fragment, a recognized privileged structure,[38] is engaged in hydrophobic interactions (Scheme 3). Finally, the switch of X = S to N was responsible for an appreciable 2-fold increase of the inhibition potency (Scheme 3).

From these results, it appeared also that the AcGs, in spite of some differences in their structural features, exhibited potency in the nanomolar range with respect to the AcUs. Moreover, as AcGs can be handled as salts, they were the preferred compounds in our hands.

Then we examined if **61** (an AcTU) and **86** (an AcG) fit the proposed pharmacophoric model for Smo antagonists described earlier.[20] The low energy conformers of **61** and **86** show a very similar orientation and fulfill all the pharmacophoric features of the model. The trimethoxy phenyl group matches both HBA1 with one of its oxygen atoms and HY1 with the aromatic moiety. The carbonyl oxygen of the acylthiourea and acylguanidine moiety corresponds to HBA2, while the carbonyl group of the amide moiety is superposed to HBA3. HY2 and HY3 are filled by the tolyl moiety and by the vicinal phenyl ring of the biphenyl substituent, respectively. On the basis of this orientation, the guanidine derivative **86** shows two hydrogen bond donor groups pointing toward a putative carboxylate moiety located on the Smo receptor instead of only one hydrogen bond donor found in the thiourea derivative **61** (Figure 2A). Two other conformers of both compounds are also able to match the model (Figure 2B). Now both compounds show two hydrogen bond donor groups pointing toward a putative carboxylate of the receptor. In addition, the conformer of **86** fitted to the model also shows an intramolecular hydrogen bond between the guanidino ═NH and the carbonyl oxygen that reduces the conformational mobility of this compound (Figure 2B and Scheme 4).

Because the electronegativity (EN) and strength of an H-bond are correlated, the ranking of the biological activities (AcG > AcU > AcTU) should follow the decreasing of the EN. Therefore the EN was assigned for each X group (Scheme 4), after Pauling's rule: for X = NH + H (AcGs), EN = 5.1, for X = O (AcUs), EN = 3.5, and for X = S (AcTUs), EN = 2.5.[39] These observations support hypotheses of H-bonds proposed in Scheme 4.

The biological activities of compounds **61**, **72**, and **86** on Shh-light2 and C3H10T1/2 cells were then compared to that of cyclopamine, GDC-0449, and Cur61414. Results are collected in Table 6, expressed as IC_{50}, and listed in order of ascending activity. The mean slope of the curves is also given for comparison.

Abnormal Shh signaling in the cerebellum of $Ptc^{\pm}$ mice has been proposed to be responsible for medulloblastoma,[40] and a higher incidence of these tumors occurs when these animals are developed on a $p53^{-/-}$ background.[41] The tumors are believed to result from a modification of the proliferative properties of the cerebellar granule cell precursors (GCPs) that populate this tissue. It has been previously demonstrated that GCPs proliferate in response to Hh pathway activation, an effect

dx.doi.org/10.1021/jm2013369 | J. Med. Chem. 2012, 55, 1559−1571

Table 5. Biological Activities of Acylguanidines

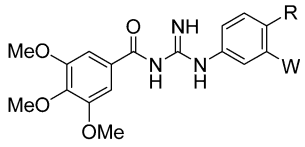

78- 91

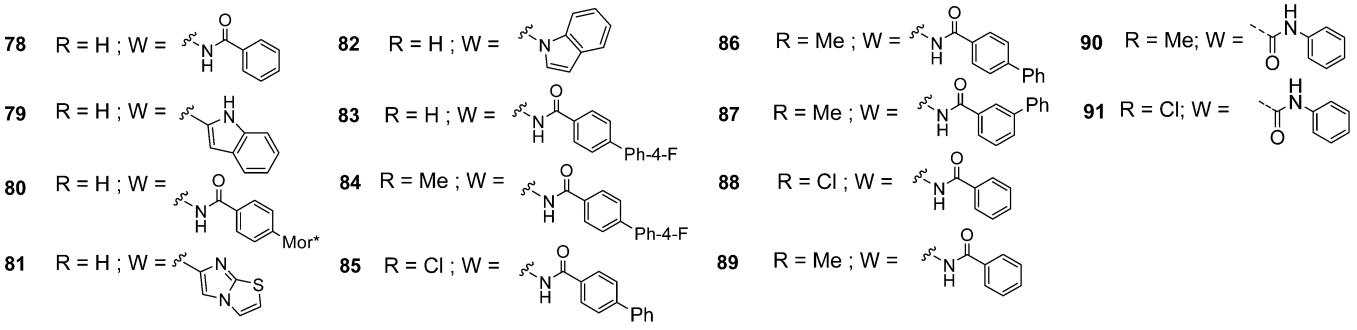

* Mor = morpholine

compd	IC$_{50}$, μM	
	Shh-light2, (Shh 5 nM)	C3H10T1/2, (SAG 0.1 μM)
cyclopamine	0.3 ± 0.05	0.62 ± 0.03
GDC-0449	0.007 ± 0.001	0.011 ± 0.001
1a	0.65 ± 0.15	0.9 ± 0.2
1b	0.16 ± 0.07	0.13 ± 0.05
78	0.29 ± 0.05	0.43 ± 0.02
79	0.07 ± 0.01	0.18 ± 0.02
80	0.22 ± 0.01	0.20 ± 0.01
81	0.64 ± 0.19	0.83 ± 0.30
82	0.90 ± 0.03	0.39 ± 0.02
83	0.033 ± 0.006	0.030 ± 0.009
84	0.014 ± 0.003	0.011 ± 0.002
85	0.07 ± 0.03	0.13 ± 0.02
86	0.015 ± 0.002	0.011 ± 0.003
87	0.11 ± 0.06	0.26 ± 0.09
88	0.37 ± 0.05	0.37 ± 0.08
89	nd[a]	0.18 ± 0.02
90	0.19 ± 0.01	0.20 ± 0.03
91	0.16 ± 0.03	0.44 ± 0.06

[a]88% inhibition at 0.3 μM.

Table 6. Comparison of Binding Affinities and Functional Potencies of Smo Inhibitors

compd	Shh-light2[a]		C3H10T1/2[a]		GCPs[b]		BC binding[c]
	IC$_{50}$, nM	n_H	IC$_{50}$, nM	n_H	IC$_{50}$, nM	n_H	IC$_{50}$, nM
1a	650 ± 150	2.0 ± 0.4	900 ± 200	1.3 ± 0.2	338 ± 34	1.6 ± 0.2	300 ± 50
cyclopamine	300 ± 50	1.6 ± 0.4	620 ± 30	1.3 ± 0.1	100 ± 6	1.4 ± 0.2	64 ± 17
Cur61414	140 ± 40	2.0 ± 0.3	300 ± 100	1.3 ± 0.2	95 ± 5	1.8 ± 0.3	nd
1b	160 ± 70	2.1 ± 0.3	130 ± 50	1.2 ± 0.1	106 ± 10	1.4 ± 0.1	107 ± 18
61	41 ± 2	2.4 ± 0.4	64 ± 15	1.2 ± 0.1	9 ± 0.1	1.6 ± 0.1	63 ± 13
72	13 ± 3	2.0 ± 0.2	25 ± 3	1.2 ± 0.1	6 ± 0.1	1.9 ± 0.3	24 ± 7
86	15 ± 2	1.9 ± 0.3	11 ± 3	1.2 ± 0.1	6 ± 1	1.6 ± 0.1	5 ± 1
GDC-0449	7 ± 1	1.7 ± 0.3	11 ± 1	1.0 ± 0.1	4 ± 1	1.5 ± 0.1	7 ± 1

[a]Shh-light2 and C3H10T1/2 tests as in Tables 1−5. [b]Granule cell precursors proliferation as determined from experiments depicted in Figure 3C. [c]BODIPY-cyclopamine (BC) binding to human Smo as determined from experiments depicted in Figure 4. IC$_{50}$ and n_H (Hill coefficient) are mean ± SEM; $n \geq 3$; nd, not determined.

inhibited by Smo antagonists.[41,42] To further investigate the antagonist properties of compounds **61**, **72**, and **86**, we analyzed their potencies to inhibit rat GCP proliferation in primary culture as measured by [^{3}H]-thymidine incorporation in comparison to other Smo antagonists including the original hits. Neither compound (1 μM) modified significantly the basal level of [^{3}H]-thymidine incorporation in rat GCPs (data not shown). As it has been previously reported, rat GCPs treatment

dx.doi.org/10.1021/jm2013369 | J. Med. Chem. 2012, 55, 1559−1571

Scheme 3. Optimization of 1a, 1b, and 78 by Discrete Structural Modifications[a]

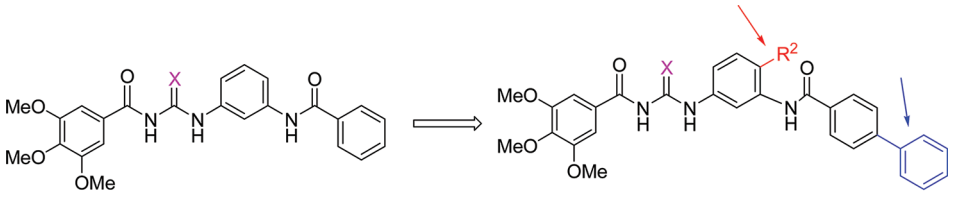

[a]Improvement came from substituents at R^2 (red) and with a second phenyl ring (blue). IC_{50} are from the C3H10T1/2 assay.

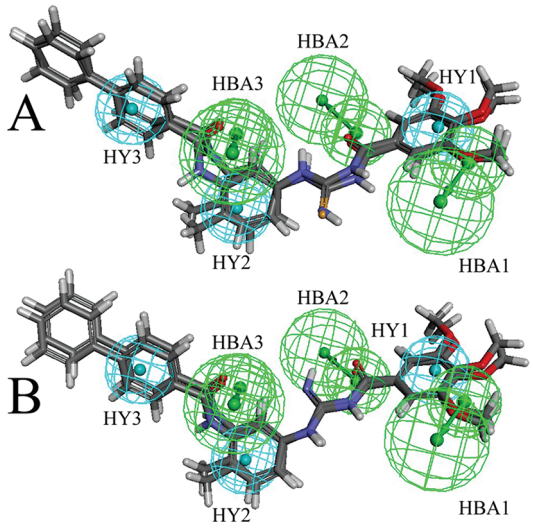

Figure 2. Compounds **61** and **86** in two different conformations layout (A,B) with the pharmacophoric model for Smo antagonists. Pharmacophoric features are color coded: green for hydrogen bond acceptor groups (HBA1−3) and cyan for hydrophobic regions (HY1−3). HBA features are constituted by a smaller sphere accommodating the hydrogen bond acceptor group, by a directionality vector represented by an arrow, and by a larger sphere intended to allocate the hydrogen bond donor group of the target macromolecule. The atoms are color coded: gray, carbon; white, hydrogen; red, oxygen; blue, nitrogen; yellow, sulfur.

with SAG causes an increase in [^{3}H]-thymidine incorporation over basal level.[43] Compounds **61**, **72**, and **86** were found to be potent antagonists of SAG (0.01 μM)-induced proliferation of rat GCPs, with an IC_{50} ranging from 6 to 9 nM (Figure 3C). Therefore, these data further validate **61**, **72**, and **86** as potent Hh inhibitors and again show that the AcU and AcG are more potent than the AcTU in this assay. The compounds were 20−60 times more potent than cyclopamine, **1a**, or Cur61414, and their IC_{50} were in the same range as GDC-0449 (Figure 1 and Table 6).[14] The Hill coefficients of the dose−response curves of the compounds presented in Table 6 were not different in the alkaline phosphatase and GCPs proliferation assays. These data suggested a similar interaction of the molecules with the receptor, whereas analysis of the slope of the concentration−response curves in the Shh-light luciferase assay indicated cooperativity (n_H ~2). Thus, these data further demonstrate that these novel series of AcTU, AcU, and AcG compounds are potent Hh pathway inhibitors.

Finally, the characterization of the mode of action of compounds **61**, **72**, and **86** was carried out by investigating whether they could compete with BODIPY-cyclopamine (BC), a fluorescent derivative of cyclopamine which interacts with Smo at the level of its heptahelical bundle.[43] We took advantage of our recent development of a BC assay on human Smo (hSmo) expressed stably in HEK293 (HEK-hSmo) cells.[44] These cells were incubated with 5 nM of BC for 2 h in the absence or presence of various concentrations of compounds (Table 6). Cyclopamine and GDC-0449 inhibited BC binding to hSmo with an IC_{50} comparable to that previously reported using a similar assay.[45] As previously observed for inhibiting BC binding to mouse Smo,[20] the hit compounds (**1a**, **1b**) demonstrated inhibition of BC binding to 423 hSmo, thus further confirming their interest for targeting the human receptor (Table 6). Compounds **61** and **72** blocked BC binding to hSmo in a dose-dependent manner with an IC_{50} of 63 and 24 nM, respectively, being notably less effective than **86** (IC_{50} of 5 nM in this test) (Figure 4). The inhibition potency of these compounds correlates well with Hh inhibition (Table 6). Altogether, these data demonstrate that **61**, **72**, and **86** are potent antagonists of human and rodent Smo receptors. These inhibitors are much larger than GDC-0449 and might potentially interact with residues well beyond the GDC-0449 binding site. Further work is needed to characterize their ligand binding site and to show if these newly disclosed inhibitors can overcome or not the GDC-0449 resistant mutations.[15,17]

CONCLUSION

In this study, the synthesis and the characterization of novel AcTUs, AcUs, and AcGs as inhibitors of Hh signaling are reported. Interestingly, the three series of compounds have a direct chemical relationship: by chemical interconversion, the AcTUs gave access to both AcUs and AcGs via a single step transformation. The AcTU **61**, AcU **72**, and AcG **86** were found as potent inhibitors as GDC-0449 in several Hh assays and in inhibiting BC binding to human Smo. Among them, the AcG **86** is an attractive compound with a balanced structure displaying two lipophilic zones at the terminal parts delineating a polar zone with an acylguanidine moiety ideal to engage H-bond interactions at the receptor level. It is worth noting that **86** (MRT-83), which does not block Wnt signaling, inhibits Hh pathway in mouse brain, suggesting this compound can block Smo in vivo.[44] Finally, these three series of compounds represent novel leads on the way to find anticancer agents[3] and they should be valuable tools for further characterizing Hh signaling and Smo pharmacology both in vitro and in vivo.

dx.doi.org/10.1021/jm2013369 | J. Med. Chem. 2012, 55, 1559−1571

Scheme 4. Proposed H-Bonding Network for the Three Bio-isosteric Structures AcTU, AcU, and AcG towards a Putative Carboxylate Located on Smo (in Agreement with the Conformations of 61 and 86 Shown in Figure 2B)

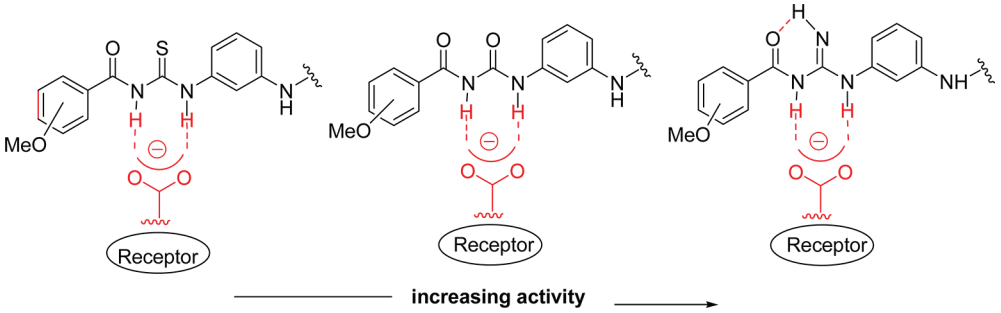

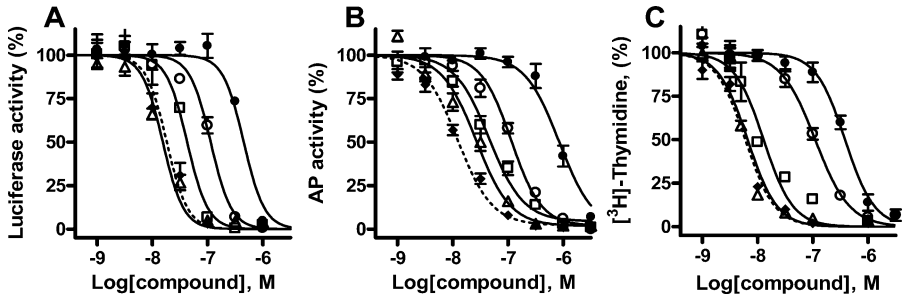

Figure 3. Dose−response inhibition curves of Shh-induced Gli-dependent luciferase activity in Shh-light2 cells (A), SAG-induced differentiation of C3H10T1/2 cells (B), or SAG-induced [^{3}H]-thymidine incorporation of rat cerebellar GCPs (C) of the tested compounds. Curves of **1a** (filled circle), **1b** (circle), **61** (square), **72** (triangle), and **86** (filled diamond and dotted line) were generated using increasing concentrations of compounds in the presence of Shh (5 nM) (A), SAG (0.1 μM) (B,) or (0.01 μM) (C). The values are expressed as % of the maximal response induced by Shh or SAG, respectively. The data are representative of independent experiments (n = 3−10) and are the means ± SEM of triplicates (A) or quadruplicates (B,C). Response curve fitting was performed with Prism software (GraphPad).

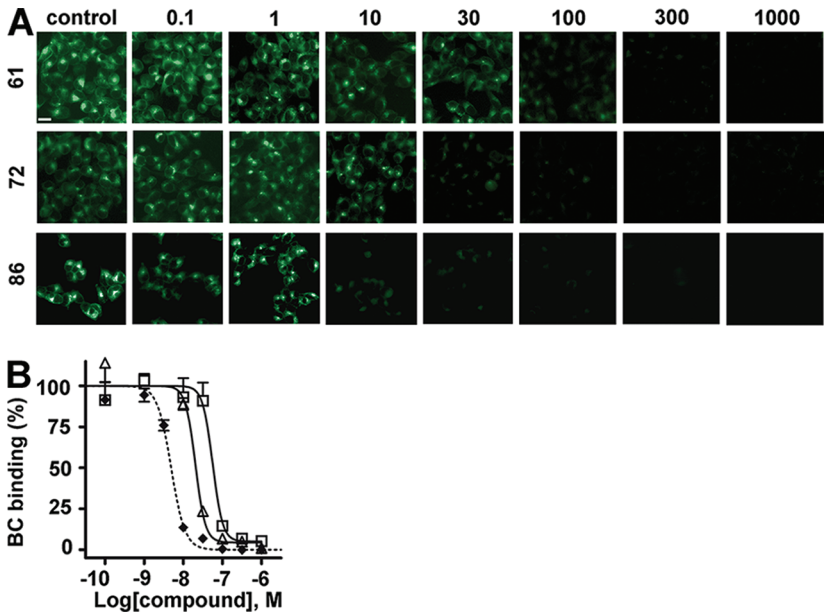

Figure 4. Inhibition of BODIPY-cyclopamine (BC) binding to HEK-hSmo cells by **61**, **72**, and **86**. (A) HEK-hSmo cells stably expressing human Smo were incubated with BC (5 nM) alone (control) or in the presence of increasing concentrations (nM) of **61** or **72**. BC binding (green) is visualized using fluorescence microscopy in a representative field (40−60 cells are shown; scale bar, 10 μm). (B) The concentration−response curves were obtained by quantification of the BC fluorescence in three photographs for each coverslip as described[44] (**61**, square; **72**, triangle; **86**, filled diamonds). The values are expressed as % of the fluorescence detected in control HEK-hSmo cells incubated with BC alone. The data are representative of independent experiments (n = 3) and are the means ± SEM of triplicates. Response curve fitting was performed with Prism software (GraphPad).

■ EXPERIMENTAL SECTION

General Procedure. All reagents were used as purchased from commercial suppliers without further purification. The reactions were carried out in oven-dried or flamed vessels and performed under N_2. Solvents were dried and purified by conventional methods prior use. The benzoylchlorides A−I were obtained from commercially available benzoic acids. Flash column chromatography was performed with Merck silica gel 60, 0.040−0.063 mm (230−400 mesh). Aluminum backed plates (Merck) precoated with silica gel 60 (UV254) were used for thin layer chromatography and were visualized by staining with

dx.doi.org/10.1021/jm2013369 | J. Med. Chem. 2012, 55, 1559−1571

$KMnO_4$. ^1H and ^{13}C spectra were recorded on Brüker (300 or 400 MHz/75 or 100 MHz) spectrometers. Chemical shifts (δ) are given in ppm relative to the resonance of their respective residual solvent peak. The chemical purity of the compounds described was determined using the following conditions: Agilent 1100 series LC/MS with a EC125/4.6 Nucleodur 100−5 C18 reversed-phase column. The binary solvent system (A/B) was as follows: 0.2% HCOOH in water (A) and acetonitrile (B). The absorbance was detected at 254 nm and the flow rate was 1 mL/min. The combustion analysis were performed by the "Service de Microanalyse, Université de Strasbourg" (France), and were within 0.5% of the theoretical values, confirming a purity of at least 95% for all tested compounds. Low resolution mass spectra were obtained on an Agilent 1100 LC/MS instrument in positive mode at the "Faculté de Pharmacie de l'Université de Strasbourg" (France). For microwave reactions, a CEM Discover microwave oven equipped with a 10 mL tube for reactions under pressure was employed.

Pharmacophoric Model of Compounds 61 and 86. We constructed a pharmacophoric model of **61** and **86** based on chemical structures of Smo inhibitors as described previously.[20] Briefly, 10 compounds were used to generate pharmacophoric hypotheses for hedgehog antagonists. Their structures were built using Catalyst 2D−3D sketcher and a representative family of conformations were generated for each molecule using the Poling algorithm and the "best conformational analysis" method. Conformations were selected that fell within a 20 kcal/mol range above the lowest energy conformation found. Each compound, with its associated conformational models, was submitted to common feature hypothesis generation (HipHop),[46] producing potential pharmacophoric models by generating alignments of common chemical features. To perform the alignment of the molecules, instead of using only the minimum energy conformers found, all the conformers generated for each compound have been included in the calculations. The chemical functions (features) used in this generation step included hydrogen bond donor (HBD), hydrogen bond acceptor lipid (HBA, it includes basic nitrogen which is not considered in the hydrogen bond acceptor feature), hydrophobic (HY), and ring aromatic (RA). The two most active compounds (Y'''' and Z'''') were used to derive common-feature based alignments and considered as "reference compounds" specifying a "Principal" value of 2. If Principal is set to 2, the chemical feature space of the conformers of such a compound is used to define the initial set of potential hypotheses. Principal equal to 1 means that this compound must map onto the pharmacophore hypotheses previously defined. A Max-OmitFeat value of 0 associated with the two reference compounds forces them to map all the features of each pharmacophore hypothesis. Principal and Max-OmitFeat values for the remaining eight compounds of the training set were set to 1 and 2, respectively.

Drugs. BODIPY-cyclopamine (BC) was from Toronto Research Chemicals Inc. (North York, Canada). SAG was synthesized as described previously.[36] Shh was from Dr D. Baker (Biogen Idec, Boston, USA). [^{3}H]-thymidine was from Perkin-Elmer (Courtaboeuf, France). SAG was dissolved in ethanol, BC in methanol, and all other compounds in DMSO at a concentration of 10 mM. First dilution was performed at 100 μM in the assay buffer and subsequent 1:10 in the same buffer. No significant influence of the vehicle (DMSO) was observed in the assays.

Cell Culture and Transfection. Zeocin, Geneticin, penicillin−streptomycin, and all cell culture media or products were from Invitrogen (Cergy Pontoise, France) except when stated. HEK293 (ATCC (Manassas, USA), CRL-1593) and C3H10T1/2 (ATCC, CCL-226) were cultured in Dulbecco's Modified Eagle's Medium supplemented with 10% fetal calf serum as described.[20] The Shh-light2 cells (from Dr P. A. Beachy, Stanford, USA) and HEK-hSmo cells stably expressing human Smo[44] were cultured in the same medium supplemented with 0.4 mg/mL Geneticin and 0.15 mg/mL Zeocin or 0.5 mg/mL Geneticin, respectively. Cells were distributed into 12-well plates containing glass coverslips coated with 0.05 mg/mL poly-D-lysine (BD Bioscience, Le Pont de Claix, France) for BC binding.

Gli-Dependent Luciferase Reporter Assay. Shh-light2 cells were incubated for 40 h with Shh (5 nM) and the studied compounds. The cell-based bioassay was performed as previously described.[20] This assay measures induced firefly luciferase and controls for nonspecific toxicity by additional measurement of constitutively expressed *Renilla reniformis* luciferase, using the ratio of these two activities.

Alkaline Phosphatase Assay. C3H10T1/2 cells were incubated for 6 days in the presence of SAG (0.1 μM) and the studied compounds. The cell-based bioassay was performed as described.[20] This is a valid assay to show biological effects of the tested compounds. It does not control for nonspecific toxicity as for the Gli-dependent luciferase assay described above.

Primary Cerebellar Cultures. Isolation of cerebellar granule cell precursors (GCPs) and quantitation of [^{3}H]-thymidine incorporation were performed as described.[44]

BC Binding. The protocol was performed as described.[44] Briefly, HEK-hSmo cells were fixed in paraformaldehyde 4% and incubated with 5 nM of BC and increasing concentrations of the studied compounds for 2 h at 37 °C. Cells were analyzed with a DMRXA2 microscope (Leica Microsystems, Nanterre, France) equipped with a Photometric Cool-Snap camera (Roper Scientific, Ottobrunn, Germany). Cell culture images were taken with a 20× objective in black and white for the analysis. BODIPY (green) and DAPI (blue) signals were analyzed in 3−4 representative fields per coverslips. Using Simple-PCI software (Hamamatsu Corporation, Massy, France), the fluorescence intensity of the cells over the basal fluorescence measured in the absence of BC was quantified and divided by the area occupied by the nuclei (DAPI staining) in the field. Data were expressed as % of fluorescence intensity observed with BC alone.

Data Analysis. Means and SEM were calculated using Excel 2003. Curve fitting and IC_{50} determinations were performed using Prism 4.03 (GraphPad software, San Diego, USA). The BC fluorescence was analyzed with the Simple-PCI software (Hamamatsu Corporation, Massy, France).

■ ASSOCIATED CONTENT

Supporting Information

Experimental chemical procedures; analytical data of compounds **20**−**91**; comparison tables of AcTU vs corresponding AcU and of AcTU vs corresponding AcG. This material is available free of charge via the Internet at http://pubs.acs.org.

■ AUTHOR INFORMATION

Corresponding Author

*Phone: +33 1 69 82 36 41. Fax: +33 1 69 82 36 39. E-mail: ruat@inaf.cnrs-gif.fr (M.R.); taddei.m@unisi.it (M.T.).

Notes

The authors declare no competing financial interest.

■ ACKNOWLEDGMENTS

This work was supported by a grant from La Ligue Contre le Cancer (Comite des Yvelines to M.R.) and the Neuropole de Recherche Francilien (doctoral fellowship 248890 to H.R.). We thank Dr. S. O'Regan for critical reading of the manuscript.

■ ABBREVIATIONS USED

Hh, Hedgehog; Ptc, Patched; Smo, Smoothened; Shh, Sonic Hedgehog; Gli, glioma-associated oncongene homologue; AcTU, acylthiourea; AcU, acylurea; AcG, acylguanidine; HMDS, hexamethyldisilazane; EDCI, 1-ethyl-3-(3-dimethylaminopropyl)-carbodiimide; GCP, granule cell precursors; BC, BODIPY-cyclopamine; h, hour; rt, room temperature

■ REFERENCES

(1) Dessaud, E.; McMahon, A. P.; Briscoe, J. Pattern formation in the vertebrate neural tube: a Sonic Hedgehog morphogen-regulated transcriptional network. *Development* **2008**, *135*, 2489−2503.

(2) Traiffort, E.; Angot, E.; Ruat, M. Sonic Hedgehog signaling in the mammalian brain. *J. Neurochem.* **2010**, *113*, 576−590.

(3) Ruat, M.; Roudaut, H.; Ferent, J.; Traiffort, E. Hedgehog trafficking, cilia and brain functions. *Differentiation* **2012**, *83*, S97−S104.
(4) Philipp, M.; Caron, M. G. Hedgehog signaling: is Smo a G protein-coupled receptor? *Curr. Biol.* **2009**, *19*, R125−R127.
(5) Barakat, M. T.; Humke, E. W.; Scott, M. P. Learning from Jekyll to control Hyde: Hedgehog signaling in development and cancer. *Trends Mol. Med.* **2010**, *16*, 337−348.
(6) Tian, H.; Callahan, C. A.; DuPree, K. J.; Darbonne, W. C.; Ahn, C. P.; Scales, S. J.; de Sauvage, F. J. Hedgehog signaling is restricted to the stromal compartment during pancreatic carcinogenesis. *Proc. Natl. Acad. Sci. U.S.A.* **2009**, *106*, 4254−4259.
(7) Nieuwenhuis, E.; Hui, C. C. Hedgehog signaling and congenital malformations. *Clin. Genet.* **2005**, *67*, 193−208.
(8) Traiffort, E.; Dubourg, C.; Faure, H.; Rognan, D.; Odent, S.; Durou, M. R.; David, V.; Ruat, M. Functional characterization of Sonic Hedgehog mutations associated with holoprosencephaly. *J. Biol. Chem.* **2004**, *279*, 42889−42897.
(9) Teglund, S.; Toftgard, R. Hedgehog: beyond medulloblastoma and basal cell carcinoma. *Biochim. Biophys. Acta* **2010**, *1805*, 181−208.
(10) Berman, D. M.; Karhadkar, S. S.; Hallahan, A. R.; Pritchard, J. I.; Eberhart, C. G.; Watkins, D. N.; Chen, J. K.; Cooper, M. K.; Taipale, J.; Olson, J. M.; Beachy, P. A. Medulloblastoma growth inhibition by Hedgehog pathway blockade. *Science* **2002**, *297*, 1559−1561.
(11) Miller-Moslin, K.; Peukert, S.; Jain, R. K.; McEwan, M. A.; Karki, R.; Llamas, L.; Yusuff, N.; He, F.; Li, Y.; Sun, Y.; Dai, M.; Perez, L.; Michael, W.; Sheng, T.; Lei, H.; Zhang, R.; Williams, J.; Bourret, A.; Ramamurthy, A.; Yuan, J.; Guo, R.; Matsumoto, M.; Vattay, A.; Maniara, W.; Amaral, A.; Dorsch, M.; Kelleher, J. F. III. 1-Amino-4-benzylphthalazines as orally bioavailable Smoothened antagonists with antitumor activity. *J. Med. Chem.* **2009**, *52*, 3954−3968.
(12) Pan, S.; Wu, X.; Jiang, J.; Gao, W.; Wan, Y.; Cheng, D.; Han, D.; Liu, J.; Englund, N. P.; Wang, Y.; Peukert, S.; Miller-Moslin, K.; Yuan, J.; Guo, R.; Matsumoto, M.; Vattay, A.; Jiang, Y.; Tsao, J.; Sun, F.; Pferdekamper, A. C.; Dodd, S.; Tuntland, T.; Maniara, W.; Kelleher, J. F.; Yao, Y.-m.; Warmuth, M.; Williams, J.; Dorsch, M. Discovery of NVP-LDE225, a Potent and Selective Smoothened Antagonist. *ACS Med. Chem. Lett.* **2010**, *1*, 130−134.
(13) Peukert, S.; Miller-Moslin, K. Small-molecule inhibitors of the hHedgehog signaling pathway as cancer therapeutics. *ChemMedChem* **2010**, *5*, 500−512.
(14) *ClinicalTrials.gov*; National Institutes of Health: Bethesda, MD; http://clinicaltrials.gov/ct2/results?term=GDC-0449 (accessed Feb 6, 2012).
(15) Rudin, C. M.; Hann, C. L.; Laterra, J.; Yauch, R. L.; Callahan, C. A.; Fu, L.; Holcomb, T.; Stinson, J.; Gould, S. E.; Coleman, B.; LoRusso, P. M.; Von Hoff, D. D.; de Sauvage, F. J.; Low, J. A. Treatment of medulloblastoma with Hedgehog pathway inhibitor GDC-0449. *N. Engl. J. Med.* **2009**, *361*, 1173−1178.
(16) Von Hoff, D. D.; Lorusso, P. M.; Rudin, C. M.; Reddy, J. C.; Yauch, R. L.; Tibes, R.; Weiss, G. J.; Borad, M. J.; Hann, C. L.; Brahmer, J. R.; Mackey, H. M.; Lum, B. L.; Darbonne, W. C.; Marsters, J. C.; de Sauvage, F. J.; Low, J. A. Inhibition of the Hedgehog Pathway in Advanced Basal-Cell Carcinoma. *N. Engl. J. Med.* **2009**, *361*, 1164−1172.
(17) Yauch, R. L.; Dijkgraaf, G. J.; Alicke, B.; Januario, T.; Ahn, C. P.; Holcomb, T.; Pujara, K.; Stinson, J.; Callahan, C. A.; Tang, T.; Bazan, J. F.; Kan, Z.; Seshagiri, S.; Hann, C. L.; Gould, S. E.; Low, J. A.; Rudin, C. M.; de Sauvage, F. J. Smoothened Mutation Confers Resistance to a Hedgehog Pathway Inhibitor in Medulloblastoma. *Science* **2009**, *326*, 572−574.
(18) Dijkgraaf, G. J.; Alicke, B.; Weinmann, L.; Januario, T.; West, K.; Modrusan, Z.; Burdick, D.; Goldsmith, R.; Robarge, K.; Sutherlin, D.; Scales, S. J.; Gould, S. E.; Yauch, R. L.; de Sauvage, F. J. Small molecule inhibition of GDC-0449 refractory Smoothened mutants and downstream mechanisms of drug resistance. *Cancer Res.* **2010**, *71*, 435−444.
(19) Buonamici, S.; Williams, J.; Morrissey, M.; Wang, A.; Guo, R.; Vattay, A.; Hsiao, K.; Yuan, J.; Green, J.; Ospina, B.; Yu, Q.; Ostrom, L.; Fordjour, P.; Anderson, D. L.; Monahan, J. E.; Kelleher, J. F.; Peukert, S.; Pan, S.; Wu, X.; Maira, S. M.; Garcia-Echeverria, C.; Briggs, K. J.; Watkins, D. N.; Yao, Y. M.; Lengauer, C.; Warmuth, M.; Sellers, W. R.; Dorsch, M. Interfering with resistance to Smoothened antagonists by inhibition of the PI3K pathway in medulloblastoma. *Sci. Transl. Med.* **2010**, *2*, 51ra70.
(20) Manetti, F.; Faure, H.; Roudaut, H.; Gorojankina, T.; Traiffort, E.; Schoenfelder, A.; Mann, A.; Solinas, A.; Taddei, M.; Ruat, M. Virtual screening-based discovery and mechanistic characterization of the acylthiourea MRT-10 family as Smoothened antagonists. *Mol. Pharmacol.* **2010**, *78*, 658−665.
(21) Hallur, G.; Jimeno, A.; Dalrymple, S.; Zhu, T.; Jung, M. K.; Hidalgo, M.; Isaacs, J. T.; Sukumar, S.; Hamel, E.; Khan, S. R. Benzoylphenylurea sulfur analogues with potent antitumor activity. *J. Med. Chem.* **2006**, *49*, 2357−2360.
(22) Okada, H.; Koyanagi, T.; Yamada, N.; Haga, T. Synthesis and antitumor activities of novel benzoylphenylurea derivatives. *Chem. Pharm. Bull. (Tokyo)* **1991**, *39*, 2308−2315.
(23) Klabunde, T.; Wendt, K. U.; Kadereit, D.; Brachvogel, V.; Burger, H. J.; Herling, A. W.; Oikonomakos, N. G.; Kosmopoulou, M. N.; Schmoll, D.; Sarubbi, E.; von Roedern, E.; Schonafinger, K.; Defossa, E. Acyl ureas as human liver glycogen phosphorylase inhibitors for the treatment of type 2 diabetes. *J. Med. Chem.* **2005**, *48*, 6178−6193.
(24) Furuta, T.; Sakai, T.; Senga, T.; Osawa, T.; Kubo, K.; Shimizu, T.; Suzuki, R.; Yoshino, T.; Endo, M.; Miwa, A. Identification of potent and selective inhibitors of PDGF receptor autophosphorylation. *J. Med. Chem.* **2006**, *49*, 2186−2192.
(25) Haynes, N. E.; Corbett, W. L.; Bizzarro, F. T.; Guertin, K. R.; Hilliard, D. W.; Holland, G. W.; Kester, R. F.; Mahaney, P. E.; Qi, L.; Spence, C. L.; Tengi, J.; Dvorozniak, M. T.; Railkar, A.; Matschinsky, F. M.; Grippo, J. F.; Grimsby, J.; Sarabu, R. Discovery, structure−activity relationships, pharmacokinetics, and efficacy of glucokinase activator (2*R*)-3-cyclopentyl-2-(4-methanesulfonylphenyl)-*N*-thiazol-2-yl-propionamide (RO0281675). *J. Med. Chem.* **2010**, *53*, 3618−3625.
(26) Keller, M.; Pop, N.; Hutzler, C.; Beck-Sickinger, A. G.; Bernhardt, G.; Buschauer, A. Guanidine−acylguanidine bioisosteric approach in the design of radioligands: synthesis of a tritium-labeled N(G)-propionylargininamide ([3H]-UR-MK114) as a highly potent and selective neuropeptide Y Y1 receptor antagonist. *J. Med. Chem.* **2008**, *51*, 8168−8172.
(27) Kleinmaier, R.; Keller, M.; Igel, P.; Buschauer, A.; Gschwind, R. M. Conformations, conformational preferences, and conformational exchange of *N*′-substituted *N*-acylguanidines: intermolecular interactions hold the key. *J. Am. Chem. Soc.* **2010**, *132*, 11223−11233.
(28) Narasimhamurthy, N.; Samuelson, A. G. Thiocarbonyl to carbonyl group transformation using CuCl and NaOH. *Tetrahedron Lett.* **1986**, *27*, 3911−3912.
(29) Shinada, T.; Umezawa, T.; Ando, T.; Kozuma, H.; Ohfune, Y. A new entry for the synthesis of *N*-acyl-*N*′-substituted guanidines. *Tetrahedron Lett.* **2006**, *47*, 1945−1947.
(30) Daga, M. C.; Taddei, M.; Varchi, G. Rapid microwave-assisted deprotection of N-Cbz and N-Bn derivatives. *Tetrahedron Lett.* **2001**, 5191−5194.
(31) Bellamy, F. D.; Ou, K. Selective reduction of aromatic nitro compounds with stannous chloride in nonacidic and nonaqueous medium. *Tetrahedron Lett.* **1984**, *25*, 839−842.
(32) Rasmussen, C. R.; Villani, J. F. J.; Weaner, , L. E.; Reynolds, B. E.; Hood, A. R.; Hecker, L. R.; Nortey, S. O.; Hanslin, A.; Costanzo, M. J.; Powell, E. T.; Molinari, A. J. Improved Procedures for the Preparation of Cycloalkyl-, Arylalkyl-, and Arylthioureas. *Synthesis* **1988**, 456−459.
(33) Yang, G.; Chen, Z.; Zhang, H. Clean synthesis of an array of *N*-benzoyl-*N*′-aryl ureas using polymer-supported reagents. *Green Chem.* **2003**, 441−442.
(34) Taipale, J.; Chen, J. K.; Cooper, M. K.; Wang, B.; Mann, R. K.; Milenkovic, L.; Scott, M. P.; Beachy, P. A. Effects of oncogenic mutations in Smoothened and Patched can be reversed by cyclopamine. *Nature* **2000**, *406*, 1005−1009.

(35) Hyman, J. M.; Firestone, A. J.; Heine, V. M.; Zhao, Y.; Ocasio, C. A.; Han, K.; Sun, M.; Rack, P. G.; Sinha, S.; Wu, J. J.; Solow-Cordero, D. E.; Jiang, J.; Rowitch, D. H.; Chen, J. K. Small-molecule inhibitors reveal multiple strategies for Hedgehog pathway blockade. *Proc. Natl. Acad. Sci. U.S.A.* **2009**, *106*, 14132−14137.
(36) Masdeu, C.; Faure, H.; Coulombe, J.; Schoenfelder, A.; Mann, A.; Brabet, I.; Pin, J. P.; Traiffort, E.; Ruat, M. Identification and characterization of Hedgehog modulator properties after functional coupling of Smoothened to G15. *Biochem. Biophys. Res. Commun.* **2006**, *349*, 471−479.
(37) Chen, J. K.; Taipale, J.; Young, K. E.; Maiti, T.; Beachy, P. A. Small molecule modulation of Smoothened activity. *Proc. Natl. Acad. Sci. U.S.A.* **2002**, *99*, 14071−14076.
(38) Hajduk, P. J.; Bures, M.; Praestgaard, J.; Fesik, S. W. Privileged molecules for protein binding identified from NMR-based screening. *J. Med. Chem.* **2000**, *43*, 3443−3447.
(39) Patel, K. M.; Patel, H. A.; Sen, D. J.; Panigrahi, B. B.; Badmanaban, R. In vitro evaluation of total reducing property of the synthesized molecule having variable atomic electronegativity. *J. Chem. Pharm. Res.* **2010**, *2*, 631−639.
(40) Goodrich, L. V.; Milenkovic, L.; Higgins, K. M.; Scott, M. P. Altered neural cell fates and medulloblastoma in mouse Patched mutants. *Science* **1997**, *277*, 1109−1113.
(41) Romer, J. T.; Kimura, H.; Magdaleno, S.; Sasai, K.; Fuller, C.; Baines, H.; Connelly, M.; Stewart, C. F.; Gould, S.; Rubin, L. L.; Curran, T. Suppression of the Shh pathway using a small molecule inhibitor eliminates medulloblastoma in Ptc1(±)p53(−/−) mice. *Cancer Cell* **2004**, *6*, 229−240.
(42) Charytoniuk, D.; Porcel, B.; Rodriguez Gomez, J.; Faure, H.; Ruat, M.; Traiffort, E. Sonic Hedgehog signalling in the developing and adult brain. *J. Physiol. (Paris)* **2002**, *96*, 9−16.
(43) Chen, J. K.; Taipale, J.; Cooper, M. K.; Beachy, P. A. Inhibition of Hedgehog signaling by direct binding of cyclopamine to Smoothened. *Genes Dev.* **2002**, *16*, 2743−2748.
(44) Roudaut, H.; Traiffort, E.; Gorojankina, T.; Vincent, L.; Faure, H.; Schoenfelder, A.; Mann, A.; Manetti, F.; Solinas, A.; Taddei, M.; Ruat, M. Identification and mechanism of action of the acylguanidine MRT-83, a novel potent Smoothened antagonist. *Mol. Pharmacol.* **2011**, *79*, 453−460.
(45) Rominger, C. M.; Bee, W. L.; Copeland, R. A.; Davenport, E. A.; Gilmartin, A.; Gontarek, R.; Hornberger, K. R.; Kallal, L. A.; Lai, Z.; Lawrie, K.; Lu, Q.; McMillan, L.; Truong, M.; Tummino, P. J.; Turunen, B.; Will, M.; Zuercher, W. J.; Rominger, D. H. Evidence for allosteric interactions of antagonist binding to the Smoothened receptor. *J. Pharmacol. Exp. Ther.* **2009**, *329*, 995−1005.
(46) Barnum, D.; Greene, J.; Smellie, A.; Sprague, P. Identification of common functional configurations among molecules. *J. Chem. Inf. Comput. Sci.* **1996**, *36*, 563−571.